AEOLIAN RIPPLE RATE VARIABILITY IN RESPONSE TO DIFFERENT BOUNDARY CONDITIONS.

S. Preston[1] and M. Chojnacki[1], [1]Lunar and Planetary Laboratory, University of Arizona, 1629 E University Blvd, 85721-0092, AZ, e-mail: spreston@email.arizona.edu.

Introduction and Motivation: Numerous factors affect aeolian bedform migration rates, such as sediment supply, wind regime, topography, elevation and interactions among neighboring bedforms [1]. Prior studies have demonstrated both meter-scale spaced ripples and larger sand dunes are migrating across Mars today but show some inconsistencies in their reported rates between the two bedform classes. [2-6]. Ripple rates have been reported as slower [2], faster [3,4], and similar to [5,6] the dunes they overlie. Reasons for these discrepancies might not just be the result of examining sites with different boundary conditions. Reported rate disparities may be caused by taking ripple measurements at different locations along the dune profile (e.g., stoss-ward side vs. crest) or sampling varying-sized ripples.

Wind velocities along dunes can be divided into three zones defined by streamwise acceleration and deceleration **(Fig. 1)** [7]. Wind speeds at the stossward (upwind) side of the dune tend to decrease due to the dune topography. Atmosphere is then compressed and accelerates leeward up the slope. Finally, wind speeds decelerate past the crest due to flow expansion. *Bridges et al.* [2] demonstrated this effect by showing a linear correlation between ripple migration and elevation along dune profiles in Nili Patera.

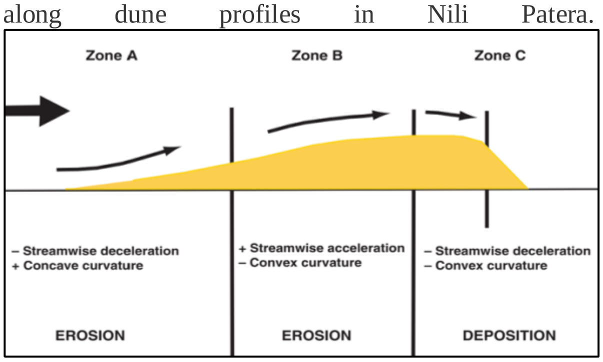

Figure 1. A diagram illustrating 3 zones of wind behavior along terrestrial dune profiles. After *Lancaster* [7].

Here, we use a more systematic approach to not only compare the migration rates between ripples and local dunes, but also to examine how ripple rates change on sand dunes moving downwind from stoss-side to lee-side. Results provide important constraints on the relative sand flux contributions of different bedforms and how terrestrial and martian bedform transport parameters compare.

Data Sets and Methods: Eight regional dune fields **(Fig. 2)** of varying geologic and environmental conditions were examined. Images taken by the High Resolution Imaging Science Experiment (HiRISE) camera (0.25-1m/pix) [8] were utilized to observe target sites. Annual monitoring images were orthorectified to parent digital terrain models [9]. To quantify these rates, Environment for Visualizing Images (ENVI) software was used to track bedform movement in orthoimages separated in time by 2-5 Mars years depending on the site and bedform type.

Measurements were primarily taken from barchan or barchanodial dunes which had similar wavelengths or spacings (200-500 m). Migration rates were measured for ten dunes per site with three ripple rates for each dune (lower-stoss, mid-dune and crest). Ripples migrating in a transverse motion (rather than oblique) were measured for this study. For dunes, three displacement measurements of the advancing slipface were taken, and then averaged to obtain migration rates.

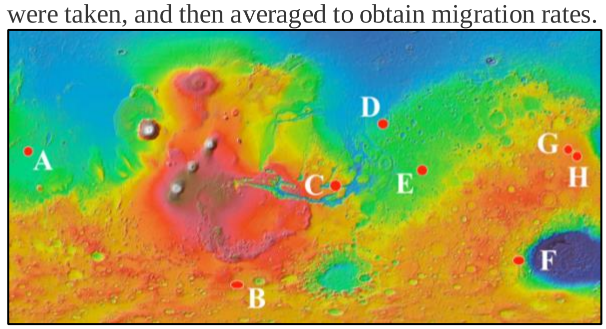

Figure 2. MOLA Global Elevation Map showing study sites: A) Cerberus, B) Coblentz, C) Ganges, D) McLaughlin, E) S. Xainza, F) Hellespontus, G) Nili Patera and H) Meroe.

Results: Average ripple rates across all three of the dune zones exhibited substantially faster migration than the local dunes at all eight measurement sites **(Table 1)**. Ripples migrated between 1-12 m/year, whereas dunes rarely exceeded 1 m/year. Ripple rates for a given site generally scaled with dune rates, as would be expected.

Table 1. Average dune and ripple migration rates from each measurement site. Ripple rate zone A represents the lower-stoss side of the dune, B the mid-dune and C adjacent to the brink.

Site	Dune Rate (m/yr)	Ripple Rate A (m/yr)	Ripple Rate B (m/yr)	Ripple Rate C (m/yr)
A - Cerberus	0.22	0.46	0.50	0.47
B - Coblentz	0.45	0.68	1.45	0.92
C – Ganges	0.37	1.12	1.40	1.24
D - McLaughlin	0.73	1.27	1.09	1.30
E – S. Xainza	0.21	1.08	1.46	1.86
F - Hellespontus	0.40	0.78	1.25	1.18

G – Nili Patera	0.66	7.44	12.19	12.80
H - Meroe	0.58	0.97	1.28	1.47

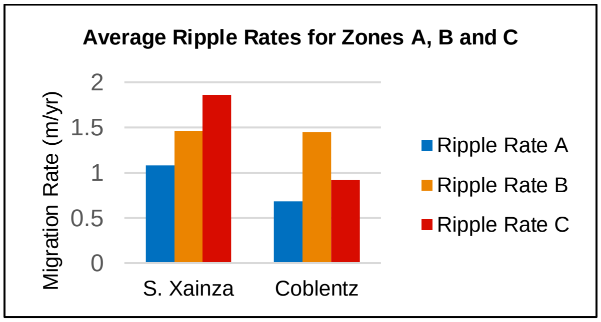

Figure 3. Two representative patterns of ripple migration rates across zones A-B-C moving stoss- to lee-side.

The slowest ripple zones (typically the upwind Zone A) were migrating 2-4 times faster than the underlying dunes, whereas the fastest zone ripples (Zone B or C) may migrate up to about 5.5 times faster.

Two distinct patterns were observed from the measured ripple rates along the dune profiles **(Fig. 3)**. The first is a stepwise pattern of increasing ripple speeds progressing downwind to the brink. The second pattern shows the slowest migration at the stoss-ward side, fastest migration at the mid-dune, and the second fastest near the brink **(Fig. 3)**.

Spatial dune profiles were taken at several sites to observe any related trends **(Fig. 4)**. Profiles taken at S. Xainza show small crest-brink separations with a sharp drop off. In contrast, Coblentz profiles illustrate much more rounded and distinct crest-brink separations.

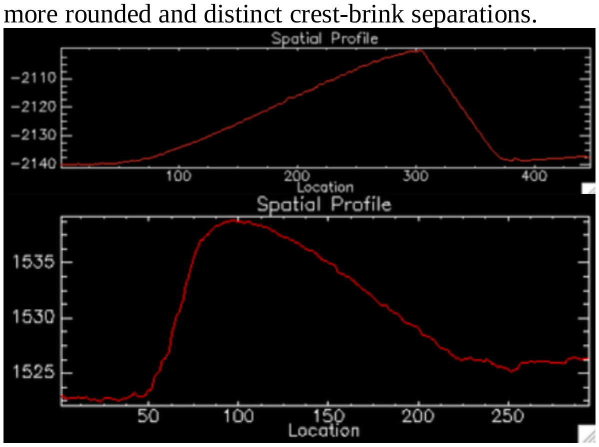

Figure 4. Spatial profiles for dunes located at S. Xainza (Top) and Coblentz (Bottom). Units are in meters.

Discussion: As described by *Lancaster* [7], terrestrial dunes exhibit three zones of differing wind velocity conditions. Wind speeds slow at the upwind toe of the dune, accelerate downwind up the slope and then decelerate once more due to flow expansion past the crest at the brink. It was expected to find a pattern consistent with this model **(Fig. 1)**, yet only half of the martian sites did **(e.g.,** Coblentz; **Fig. 3**). 4 of the 8 sites expressed ripple patterns more like S. Xainza **(Fig. 3)**.

We believe the reason for these differing ripple velocity patterns illustrated in **Fig. 3** are the result of a combination of varying crest-brink separation sizes as well as elevation differences between the crest and brink. This is caused by a difference in morphology, topography and/or local wind patterns.

Some dune morphologies are such that the crests or apexes are very near the slipface brink and no rollover occurs (e.g., S. Xainza). These dunes showed greater elevations and rates for zone C ripples, the latter due to streamwise acceleration. Underlying topography may cause dunes climbing upslope to have a crest and brink of similar elevation (e.g. Hellespontus). This would mean that the ripple migration rates would not vary much between the crest and brink, assuming *Bridges et al.'s* [2] linear relationship between ripple migration and dune height [6]. The local wind regime may also affect the size of this crest-brink separation. Dunes that are consistently moved along the same direction will be developed more sharply at their slipface.

Conclusion: Ripples are observed to be moving much faster than the dunes they superimpose. The relative speeds at which these ripples move along the dune profile relates to topography, wind regime and/or resulting dune morphology. Climbing dunes or dunes of certain morphology may have a crest and brink of similar elevation. This would mean that the zone of streamwise deceleration located at the brink may not be detectable. Crest brink separation sizes may vary as a result of the local wind regime. If the separation is too small this will also affect the detectability of the downwind zone of streamwise deceleration in our measurements. Any combination and differing degree of both of these factors exist at all sites depending on the individual dune and its location.

Acknowledgments: This research was supported in part by NASA MDAP Grants NNH14ZDA001N and the HiRISE/MRO mission. We would like to thank UofA students and staff for assistance with targeting and DTM production.

References: [1] G.A. Kocurek and R. Ewing (2012) in *Sediment. Geol. of Mars*, J.P. Grotzinger, Ed. [2] N.T. Bridges et. al. (2012) *Nature*, 485, 339-342. [3] S. Silvestro (2013) *Geol.*, 41, 483-486. [4] K.D. Runyon et. al. (2017) *Aeolian Res.* 29, 1–11. [5] M.E. Banks et. al. (2011) *JGR Planets*, 2018JE005747. [6] N.T. Bridges et. al. (2011) *Geol.*, 40, 31-34. [7] N. Lancaster, in *Geomorph. of Desert Enviro.,* A.J. Parsons Ed. (Springer, 2009). [8] A.S. McEwen, *JGR Planets*, 112 (2007), 2005JE002605. [9] M. Chojnacki et al. (2018) *JGR Planets,* 2017JE005460. [10] S. Silvestro et. al. (2016) *GRL*, 2016GL070014.